Landform Analysis, Vol. 17: 57–63 (2011)

Evolution of rill networks on soil-mantled experimental landscapes driven by rainfall and baselevel adjustments

Lee M. Gordon[1], Sean J. Bennett[1], Robert R. Wells[2]

[1]*Department of Geography, University at Buffalo, Buffalo, New York, USA, e-mail: lmg@nyserda.org*
[2]*USDA-ARS, National Sedimentation Laboratory, Oxford, Mississippi, USA e-mail: robert.wells@ars.usda.gov*

Abstract: Experiments were conducted using a soil-mantled flume subjected to simulated rain and downstream baselevel lowering to quantify the evolution of rill networks. Results show that: (1) headcuts formed by baselevel lowering were the primary drivers of rill incision and network development, and the communication of this wave of degradation occurred very quickly through the landscape, (2) rill networks extended upstream by headcut erosion, where channels bifurcated and filled the available space, (3) rill incision, channel development, and peaks in sediment efflux occurred episodically, linked directly to the downstream baselevel adjustments, and (4) sediment discharge and rill drainage density approached asymptotic values with time following baselevel adjustments despite continuous application of rainfall. These findings have important implications for the prediction of soil loss, rill network development, and landscape evolution where headcut erosion can occur.

Keywords: rill erosion, rill networks, headcuts, simulated rainfall, digital elevation models

Introduction

Soil erosion is a critical concern for the sustainable management of agricultural regions within the U.S. and worldwide. Soil erosion is the principal cause of soil degradation, and off-site impacts of sedimentation can severely affect water quality, ecology, and ecological habitat (Pimentel et al. 1995, Lal 2001). Concentrated flow erosion, specifically the growth and development of rills and gullies, then becomes the focus of this degradation, since these channels may be the dominant sources of sediment within their watersheds (Poesen et al. 2003).

Various mechanisms have been suggested to explain the formation of rills. These include: (1) a critical slope-length for soil bed incision, (2) a threshold shear stress, stream power, or slope for soil bed incision, (3) the existence of seepage erosion and exfiltration, (4) overland flow hydraulics, and (5) headcut development and migration (e.g., Savat & De Ploey 1982; Torri et al. 1987; Slattery & Bryan 1992; Huang et al. 2001; Yao et al. 2008), among others. While these mechanisms need not be mutually exclusive, all can be considered internal to the system (endogenically-forced). In contrast, studies that consider the growth and development of rill networks using relatively large physical models rely upon a rill formation mechanism external to the system (exogenically-forced), specifically baselevel lowering (Parker 1977; Gardner 1983). This baselevel adjustment produces a localized headcut that is communicated upstream, bifurcating as it does so to create a rill network, or incising and enhancing a preexisting drainage pattern. While the importance of headcut erosion in rill and gully development is receiving increased attention (Bennett et al. 2000), this discrete scour process has not been extensively studied in an experimental landscape where channel width is unconfined and where rill networks can freely develop. Moreover, the link between network development, sediment efflux, and rill erosion processes over time and space remain poorly defined, primarily because the requisite data have not yet been collected.

The primary goal of this research program is to define the processes of rill formation and network development within a soil-mantled landscape subjected to an exogenically-forced perturbation (baselevel lowering). The primary objectives of this study were: (1) to develop a comprehensive dataset

of rill network evolution in an experimental landscape subjected to simulated rain and episodic baselevel lowering with a very high temporal and spatial resolution, (2) to define the relationship between rill network development and sediment efflux using direct and indirect sampling methods, and (3) to quantitatively define the response of a soil-mantled landscape over time and space to this exogenic forcing and its effect on the evolving rill network system.

Methods

Flume and Rainfall Simulator

Experiments were conducted in a 7.0 m × 2.4 m flume (16.38 m^2, Fig. 1) housed within the Geomorphology Laboratory of the University at Buffalo. The flume is set at a 5% slope, has 0.3-m high sidewalls, and has diversions at the downstream end of the flume to direct runoff through a 0.16 m weir. The weir is fully adjustable so that baselevel with respect to the soil bed can be modified during an experiment. The bottom of the flume is perforated and covered with layers of pea gravel and landscape fabric to facilitate free drainage of the soil bed. Simulated rainfall is delivered by four cone-jet nozzles (Lechler 460.848.30BK) at a mean fall height of 3.5 m. Municipal water is pumped to each of the nozzles at approximately 10 PSI. A similar rainfall simulator produced about 75% of the kinetic energy equivalent of natural rainfall (Brunton & Bryan 2000). Rainfall rates were measured at 250 raingauges (mean gauge spacing of 0.25 m) arranged in a grid pattern within the flume prior to each experimental run. Rainfall rates averaged 87 mm hr^{-1} with a standard deviation of 31 mm hr^{-1}.

Fig. 1. Experimental landscape facility, University at Buffalo showing rainfall nozzles, camera track, flume and soil bed, and sample collection weir. Flume is 7.0 m long and 2.4 m wide, and flow is from top to bottom

Soil Material and Landscape Preparation

The *Ap* horizon of the Cheektowaga fine sandy loam from northern Erie County in western New York State is used here, chosen for its propensity to exhibit surface sealing characteristics conducive to headcut development and rill erosion. Soil was air dried to a moisture content of ~5%, mechanically crushed, and sieved at 2 mm to remove gravel and large organic material. The prepared bulk soil material consisted of 20% clay, 22% silt, and 58% sand. Soil was added to the flume in layers up to 0.04 m thick and shaped incrementally to create a broad central depression representative of a natural drainage basin in the downstream half of the flume (Fig. 1). Final soil depths were ~0.22 m at the flume periphery and ~0.14 m along the central depression. Initial bulk density was 1,380 and 1,360 kg m^{-3} for Runs 4 and 5 presented here, respectively. During each experiment, several shear strength measurements of the surface layer were made at the upstream end of the flume where the soil bed was not disturbed by concentrated flow erosion.

Rainfall Application and Sediment Sampling

A total of 15 and 20 rainstorms were applied during Runs 4 and 5, respectively. The first rainstorms applied to dry soil beds lasted 85 min. After the initial wetting storm, the baselevel at the weir was dropped by 0.03 m, creating a preformed step in bed elevation at the flume outlet. Following baselevel change, storms were limited to 15 to 30 min, as rates of rill erosion, network development, and sediment discharge initially were high. As the landscapes reached steady-state conditions, storm durations were increased to approximately 60 to 120 min. During each storm, rates of runoff and sediment discharge were measured at the flume outlet at an interval equal to approximately one third of storm duration. Captured in 1.0 l containers, sediment samples were weighed, decanted, and oven-dried, and runoff rates were measured by weighing a 30 s sample.

Digital Photogrammetry

A 10 Mp Canon EOS 20D digital camera was mounted to a movable carriage on a rail system suspended about 3.4 meters above the soil bed. Before each storm, a series of nine overlapping photographs encompassing the entire soil surface were acquired along the longitudinal axis of the flume. The camera position was advanced 0.8 m for each photograph, resulting in an average overlap for neighboring images of 67%. Fifty photogrammetric control targets with a spacing of approximately 0.3 m were secured to the top edge of the flume sidewall. These targets were surveyed by a Pentax PCS-1s (1 s angular resolution) Electronic Total Station from two fixed locations near the downstream end of the flume. Bearings (horizontal and vertical angles) to the targets from the two stations were converted to three-dimensional coordinates using intersection and triangulation methods as described by Chandler et al. (2001). These control coordinates, interior and exterior camera orientation information, and lens distortion model parameters were linked to 8 image pairs within the Leica Photogrammetry Suite (LPS) v. 9.2 software. An average of 6 control points were manually identified within each image pair and 150 radiometrically and/or geometrically similar tie points were identified automatically. These points then were used to obtain a triangulated solution for each image pair. A single digital elevation model was generated for each image pair at a cell size of 3 mm. The LPS Mosaic Tool then was used to produce a full-field DEM of the entire flume. Uncertainties from all sources (surveying, control point digitizing, triangulation, and DEM interpolation) produce combined errors on the order of 1 to 3 mm.

Results

Rainfall Application and Landscape Response

After landscape preparation, with the terminal weir spillway set at the height of the soil bed, 85 minutes of rainfall was applied. After ~5 min, ponding was observed as the soil surface became saturated. Initial runoff occurred at ~10 min and averaged 7.0, 11.0, and 14.8 l min^{-1} at 20, 45, and 75 minutes, respectively. The wetting front was observable through the flume sidewalls, and it progressed quickly through the soil bed, reaching the bottom of the flume during the first simulated storm. At the soil surface, raindrop impact and sheetflow caused a thin pliable surface seal to form as aggregates were dispersed and fines were washed into voids. In the broad central thalweg, approximately one meter upstream of the weir, bed scour began in the form of a very shallow (<10 mm) headcut. This initial headcut migrated upstream at a constant scour depth and expanded laterally to create a continuous wide shallow scarp, which continued to expand throughout the majority of the experiment.

At the conclusion of the initial wetting storm, the terminal weir was lowered 0.3 m. This resulted in a preformed step at the flume outlet measuring 0.16 m wide and 0.03 m high. At the start of the second storm, runoff occurred almost immediately, passing over the preformed step at the outlet, eroding the face of the step and causing the step face to quickly retreat upstream into the flume. As the step migrated upstream along the path of concentrated flow, it took the form of an arcuate-shaped headcut with a vertical face (Fig. 2). As the primary headcut (designated Type 1) passed the center portion of the flume, it encountered the transition between the broad central depression (thalweg) and the upland hillslope. At this transition, the primary headcut tended to bifurcate into lower order tributary headcuts (designated Type 2, Fig. 2). Concurrently, in the downstream half of the flume, other headcuts were initiated within the preexisting primary channel (designated Type 3). Type 3 headcuts propagated throughout the network and into preexisting tributaries (designated Type 4, Fig. 2) in semi-regular waves of degradation. While Type 1 and 2 headcuts propagated directly from the pre-existing step at the baselevel drop, Type 3 and 4 headcuts were generated at channel confluences and at small undulations in the channel bed where locally high shear stresses might be expected.

Sediment Signatures and Steady State Erosion

Both experimental runs were dominated by supply-limited flow regimes. Very little deposition was observed and this typically consisted of fan-like accumulation in the extreme downstream end of the flume as conditioned by the terminal weir. Cumulative sediment efflux S_{TOT} measured at the flume outlet provides an opportunity to validate volumetric DEM-derived sediment budgets.

Experimental observations indicated that two adjustments were necessary to match the sampled sediment efflux with calculations made using the DEMs. First, a linear correction was applied to the DEM volumes over the duration of the experiment to account for the increase in bulk density of the soil bed throughout the experiment. Second, a correction was made between the initial surface DEM and the DEM acquired after the first wetting storm to account for a flume-wide settling (~17 mm) of the soil bed foundation (fabric and gravel layers) that occurred during the first simulated rainstorm. The need for these corrections was experimentally verified by the significant increase in the observed bed shear strength of the soil (not shown here). Figure 3

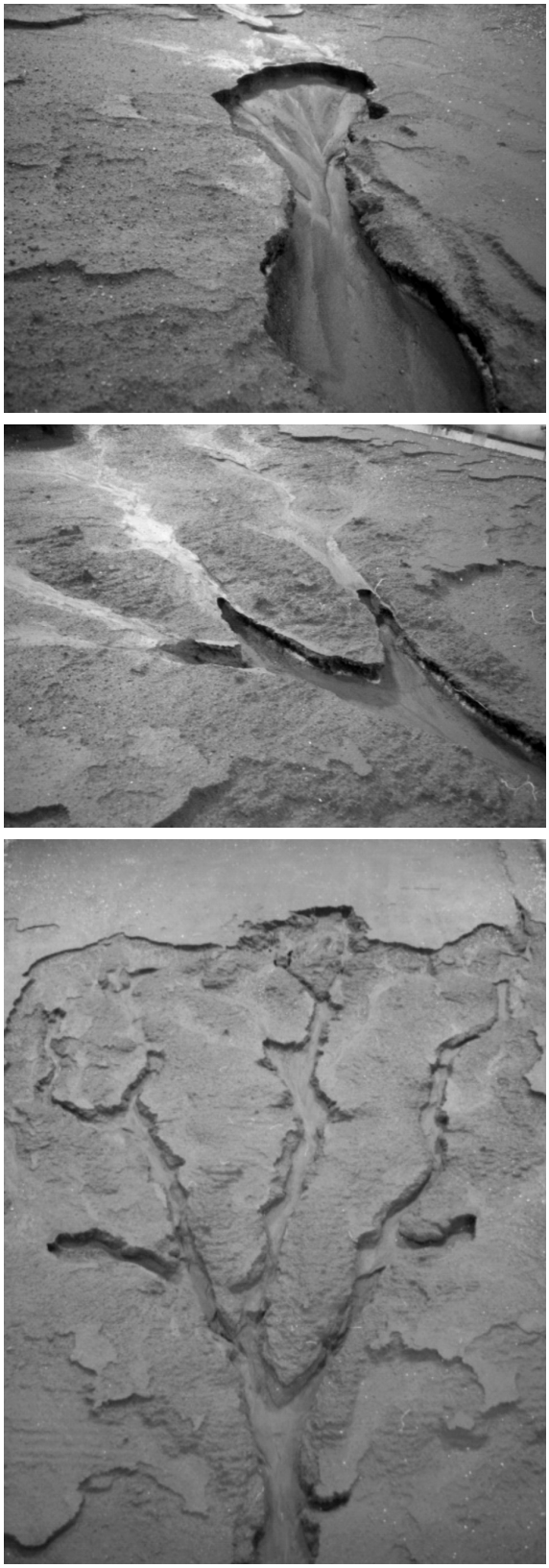

Fig. 2. Representative photographs of the headcut forms observed (from top to bottom): Type 1 primary headcut resulting directly from drop in baselevel; bifurcation of Type 1 primary headcut into three Type 2 tributary headcuts; and network of tributary rill channels dominated by Type 4 tributary headcuts and bounded upstream by the initial scarp. Beds are several decimenters to two meters in width

indicates excellent agreement between the measured sediment efflux and that calculated and corrected using the DEMs.

Sediment discharge at the flume exit S_Y was minimal during the initial wetting storm, peaking after the baselevel reduction created the first primary headcuts (Fig. 3). Sediment discharge asymptotically decreased to a quasi-steady state after approximately 250 min. This steady state was maintained until a second baselevel reduction was administered (at 842 min in Run 5) or the experiment was terminated (at 775 min in Run 4). When a second baselevel drop of 0.03 m (for a total drop of 0.06 m) was applied in Run 5, sediment discharge again spiked (Fig. 3), but quickly resumed the asymptotic reduction observed earlier in the experiment. Erosion rates after the second baselevel drop were comparable to those following the initial baselevel drop.

Network Development

To objectively define a drainage network in a rapidly evolving landscape where flows become braided

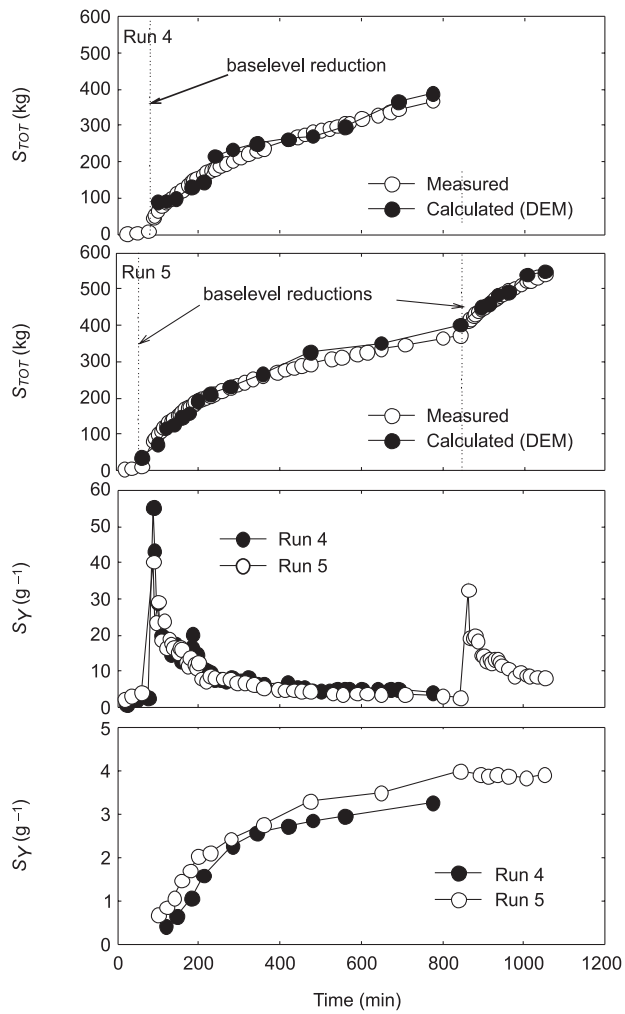

Fig. 3. Time series variations in cumulative sediment efflux S_{tot} for Run 4 and Run 5, instantaneous sediment discharge S_Y, and rill drainage density D_D

and/or transient is difficult. The DEMs collected here provide a means of defining and assessing this drainage network objectively, accurately, and quickly. The following method was used to define the rill network (i.e. 1-D lines representing rill thalwegs). First, DEM cells with a contributing area of 2000 cells (0.018 m^2) were delineated as the flow network. Second, any segment of the flow network that was not representative of a location on the soil bed that had incised at least 0.02 m was eliminated from the defined rill network. Due to the nature of the headcut-driven erosion in these experiments and the expansion of the initial outer scarp, the resulting rill network matched nicely with the erosional features observed in the orthophotographs (not shown here). The time series plots of drainage density D_D (total rill channel length divided by total drainage area; Fig. 3) follow the trends in cumulative sediment discharge, initially increasing rapidly, but attaining a quasi-steady state after approximately 250 min. After the second baselevel drop at ~850 min for Run 5, however, sediment efflux continues to increase while drainage density remains relatively constant.

Headcut Erosion

Virtually all sediment eroded within this evolving rill network occurred as a result of migrating headcuts. This could be accurately assessed by subtracting successive DEMs and noting the occurrence and migration of the headcuts (not shown here). There was no erosion of the preexisting drainage network either upstream or downstream of the areas of headcut activity, and there was minimal erosion as the outer scarp (also a headcut) retreats. Once the headcuts have migrated through, the nearly vertical channel walls were slowly obliterated due to rainsplash and lateral retreat due to sheetflow. Thus all soil erosion within this rill network could be genetically linked to headcut development and migration.

Headcut migration rate was not significantly correlated to scour pool depth, distance from the flume outlet, time following baselevel drop, or drainage area (Fig. 4). The correlation was not significantly improved by plotting the migration rates of individual headcut types (Types 1 to 4) for these same parameters. It is clear, however, that the initial headcut steps formed by baselevel drop migrated much faster (up to two orders of magnitude) than those headcuts developed as tributaries or within pre-existing channels. For all headcuts measured, Type 1, 2, 3, and 4 headcuts migrated on average at 0.94, 0.10, 0.45, and 0.15 mm s^{-1}, respectively.

When examining cumulative total incision (the elevation change between the initial pre-experiment topography and the bottom of the scour pool of the headcut of interest) at migrating headcuts, it is clear that the system continued to adjust to the depth of baselevel drop, in both space and time (Fig. 5). That is, following a baselevel drop of 0.03 m, regardless of

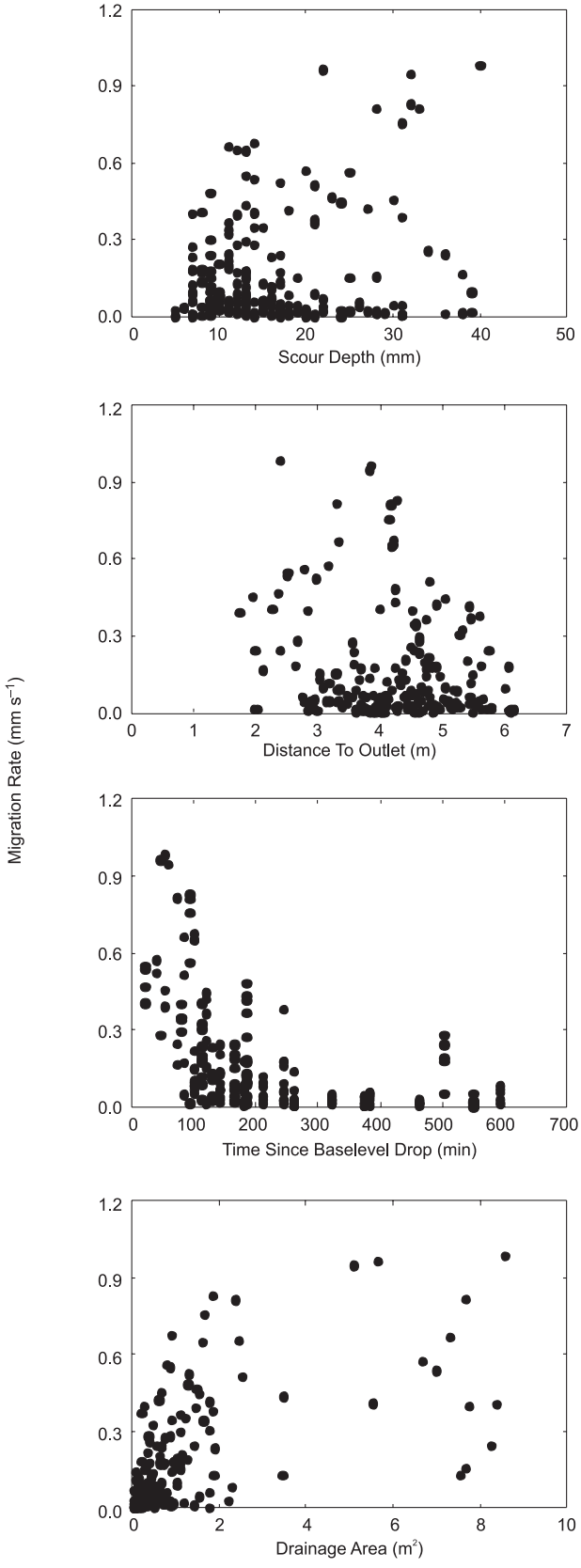

Fig. 4. Headcut migration rate as a function of scour pool depth, distance from the flume outlet, time after baselevel drop, and drainage area

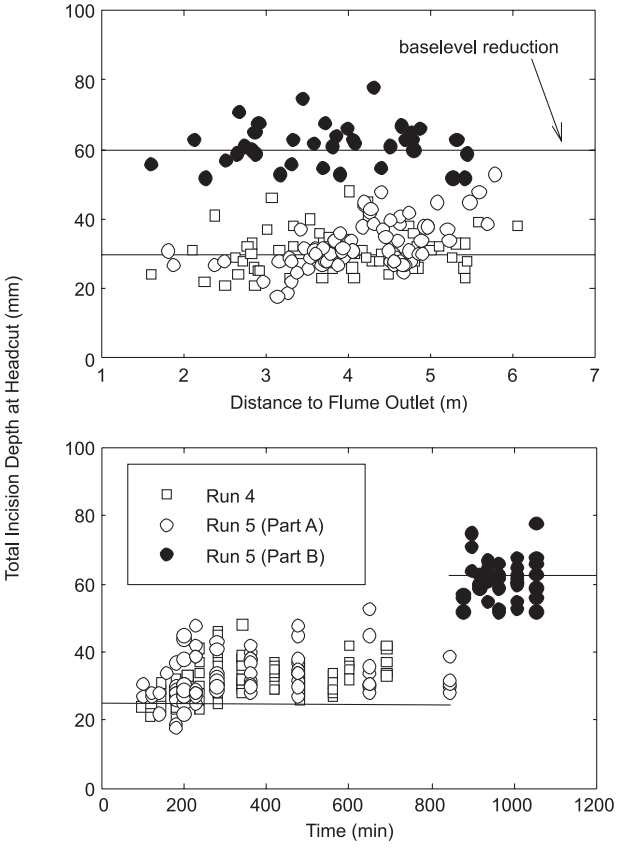

Fig. 5. Total depth of incision measured within headcut scour holes as a function of distance to flume outlet and time. For Run 5, headcuts in Parts A and B correspond to first and second baselevel drops, respectively

how much time had passed or where in the network a particular headcut was located, the cumulative erosion depth tended to mirror the baselevel drop. When the second baselevel drop was applied in Run 5, the depth of erosion throughout the landscape tended towards the ~0.06 m baselevel. Thus, the exogenically-forced perturbation placed on the system was quickly and effectively communicated to all portions of the evolving rill network.

Discussion

Exogenic Forcing and Rill Erosion

During preliminary experimentation, for the boundary conditions presented herein, virtually no erosion occurred in the absence of a baselevel drop. For this slope and topographic configuration, the soil material and preparation procedures resulted in a very stable initial condition. The system required an external forcing–baselevel lowering–to provide sufficient potential energy to erode the landscape. As the initial headcut retreated from the flume outlet, it incised a primary central rill channel whose depth pinched out in the upstream direction, and bifurcations and tributary channels formed concomitantly but at much lower rate of headward advance. Thus network development occurred here was similar to the process described by Howard (1971), wherein channels grow headward and bifurcate, filling the available space.

Rill incision and network development is intimately related to headcut erosion. While four types of headcuts were observed here, the fastest moving features were those formed by baselevel lowering. These exogenically–forced headcuts were communicated quickly and efficiently throughout the network system, and nearly all sediment efflux was genetically linked these to scour processes.

Episodic adjustment and steady-state erosion

Rill incision, channel development, and sediment efflux occurred episodically in time, related directly to the imposed baselevel adjustments. While these rapidly-migrating headcuts caused rill incision and spikes in sediment efflux, the secondary waves of degradation driven by the minor headcuts were not expressed in the sediment discharge time series. Sediment efflux and drainage density approached nearly constant or asymptotic values for most the experiments, despite the continuous application of rainfall. Thus sediment efflux and rill network development achieved steady-state erosion conditions similar to the declining equilibrium landscape of Hancock & Willgoose (2001) when the system was not perturbed by the downstream baselevel control.

Conclusions

Soil loss due to rill and gully erosion remains a critical concern in agricultural regions, since these processes can lead to significant ecologic and landscape degradation. Experiments were conducted to examine the processes of soil erosion and rill network development in the presence of simulated rain and changes in the downstream baselevel control. These experiments showed that significant soil erosion, bed incision, and rill network growth occurred quickly and pervasively when the downstream baselevel was lowered, forming an actively migrating headcut. Following this wave of degradation, both sediment efflux decreased markedly and further rill network development was halted. For the boundary conditions used here, nearly all soil loss could be attributed to migrating headcuts, and in particular those formed during baselevel adjustments. Thus by controlling such exogenic perturbations, soil-mantled landscapes can remain relatively stable with very low rates of soil loss even in the presence of continuous, high-intensity rainfall for relatively long periods of time.

References

Bennett S.J., Alonso C.V., Prasad S.N. & Römkens M.J.M., 2000. An experimental study of headcut growth and migration in upland concentrated flows. *Water Resourc. Res*. 36: 1911–1922.

Brunton, D.A. & Bryan R.B., 2000. Rill network development and sediment budgets. *Earth Surf. Proc. Landf*. 25: 783–800.

Chandler J.H., Shiono K., Ponnambalam R.& Lane S., 2001. Measuring flume surfaces for hydraulics research using a Kodak DCS460. *The Photogram. Record* 17: 39–61.

Gardner T.W., 1983. Experimental study of knickpoint and longitudinal profile evolution in cohesive, homogenous material. *Geol. Soc. Am. Bull*. 94: 664–672.

Hancock G.R. & Willgoose G.R., 2001. Use of a landscape simulator in the validation of the SIBERIA catchment evolution model: declining equilibrium landforms. *Water Resourc. Res*. 37: 1981–1992.

Howard A.D., 1971. Simulation of stream networks by headward growth and branching. *Geog. Anal*. 3: 29–50.

Huang C., Gascuel-Odoux, C. & Cros-Cayot, S., 2001. Hillslope topographic and hydrologic effects on overland flow and erosion. *Catena* 46: 177–188.

Lal R., 2001. Soil degradation by erosion. *Land Degrad. Dev*. 12: 519–539.

Parker R.S., 1977. *Experimental study of basin evolution and its hydrologic implications*. Ph.D. thesis, Colo. State Univ., Ft. Collins.

Pimentel D., Harvey C., Resosudarmo P., Sinclair K., Kurz D., McNair M., Crist S., Shpritz L., Fitton L., Saffouri R. & Blair R., 1995. Environmental and economic costs of soil erosion and conservation benefits. *Science* 267: 1117–1123.

Poesen J., Nachtergaele J., Verstraeten G. & Valentin C., 2003. Gully erosion and environmental change: importance and research needs. *Catena* 50: 91–133.

Savat J. & DePloey J., 1982. Sheetwash and rill development. *In*: Bryan, R.& Yair, A. (*Eds*.) *Badland Geomorphology and Piping.* Geobooks, Norwich: 113–126.

Slattery M.C. & Bryan R.B., 1992. Hydraulic conditions for rill incision under simulated rainfall: a laboratory experiment. *Earth Surf. Proc. Landf*. 17: 127–146.

Torri D., Sfalanga M. & Chisci F.G., 1987. Threshold conditions for incipient rilling. In: Bryan, R.B. (ed.) *Rill Erosion: Processes and Significance*. Catena-Verlag, Catena Supplement 8, Germany: 97–105

Yao C., Lei T., Elliot W.J., McCool D.K., Zhao J. & Chen S., 2008. Critical conditions for rill initiation. *Trans., Am. Soc. Agric. and Biol. Engrs*. 51: 107–114.